Journal of Orthopaedic Translation 28 (2021) 159–168

Contents lists available at ScienceDirect

Journal of Orthopaedic Translation

journal homepage: www.journals.elsevier.com/journal-of-orthopaedic-translation

3-D microarchitectural properties and rod- and plate-like trabecular morphometric properties of femur head cancellous bones in patients with rheumatoid arthritis, osteoarthritis, and osteoporosis

Ming Ding [a,*], Søren Overgaard [a,b]

[a] Orthopedic Research Laboratory, Department of Orthopedic Surgery & Traumatology, Odense University Hospital, And Department of Clinical Research, University of Southern Denmark, 5000, Odense, C, Denmark
[b] Department of Orthopaedic Surgery & Traumatology, Copenhagen University Hospital, Bispebjerg, And Department of Clinical Medicine, University of Copenhagen, 2400, Copenhagen, NV, Denmark

ARTICLE INFO

Keywords:
Rod- and plate-like trabeculae
Microarchitectural properties
Rheumatoid arthritis
Osteoarthritis
Osteoporosis
Mechanical properties

ABSTRACT

Objectives: We quantify 3-D microarchitectural properties of femoral head cancellous bones from patients with rheumatoid arthritis (RA, n = 12), osteoarthritis (OA, n = 15), osteoporosis (OP, n = 24), or donor controls (CNT, n = 8); and investigate their rod- and plate-like trabecular morphometric properties of trabecular bone tissues and compare these properties between them.

Methods: Femoral heads were harvested during total hip replacement surgeries or collected from donors. Four cubic cancellous bone samples produced from each femoral head were micro-CT scanned to quantify their microarchitectural and rod- and plate-like trabecular properties. The samples were then tested in compression to determine mechanical properties.

Results: The microarchitectural properties of femoral head cancellous bone revealed significant differences among the 4 groups, but not between RA and OA. Bone volume fraction was significantly greater in the RA and the OA than in the OP and the CNT. Structure model index was significantly lower in the RA and the OA than in the OP. Number of rods in the RA was significantly greater than in the other 3 groups. Number of plates and plate volume density in the RA and the OA were significantly greater than in the OP and the CNT. Mechanical properties were significantly greater in the RA and the OA than in the OP. The single best determinant for mechanical properties was bone volume fraction.

Conclusions: This study demonstrates significant differences in 3-D microarchitectural properties and rod- and plate-like trabecular morphometric properties among patients with RA, OA, or OP. The RA and OA cancellous bones displayed similar patterns of microarchitectural degeneration and pronounced different microarchitectures from the OP. The OP group revealed the weakest cancellous bone strength, while the RA and OA groups exhibited a compensatory effect that maintains bone tissues, and hence mechanical properties.

The translational potential of this article: The study enhances the understanding of microarchitectural degeneration of diseased cancellous bone. The OP group had the weakest cancellous bone strength, while the RA and OA groups exhibited a compensatory effect that maintains bone tissues, and hence mechanical properties. These results are particularly important for design and survival of joint prosthesis.

1. Introduction

Rheumatoid arthritis (RA), osteoarthritis (OA), and osteoporosis (OP) are the most common bone diseases worldwide, causing major public health problems in terms of pain, reduced physical activity, quality of life, and increased mortality leading to enormous economic cost [1–3]. RA is a highly bone destructive disease leading to bone erosion, and it is frequently associated with both para-articular and generalized osteoporosis [4]. OA is an age-related degenerative disease characterized pathologically by focal areas of articular cartilage loss associated with varying

* Corresponding author. Professor Orthopedic Research Laboratory Department of Orthopedic Surgery & Traumatology Odense University Hospital J.B. Winsloewsvej 15, 3rd floor, 5000, Odense, C, Denmark.
E-mail address: ming.ding@rsyd.dk (M. Ding).

https://doi.org/10.1016/j.jot.2021.02.002
Received 13 December 2020; Received in revised form 28 January 2021; Accepted 3 February 2021

degrees of osteophyte formation, subchondral bone change, sclerosis, and synovitis [2]. OP is a multifactorial disorder associated with low bone mass and enhanced skeletal fragility [5,6].

These diseases have abnormal bone remodeling characterized by an imbalance between bone resorption and bone formation. In RA, systemic and local factors disrupt the process of physiologic bone remodeling. Local microenvironment and mechanical forces, cell types, and inflammation have very different effects on bone, often resulting in bone loss in joints and in periarticular and systemic bone in RA. The inhibition of osteoblast-mediated bone formation limits erosion repairs in the RA joint [7,8]. In OA, early bone loss due to increased bone remodeling is followed by slow turnover that induces subchondral plate densification and the complete loss of cartilage at the late stage. Decreased bone resorption occurring without a decreased bone formation and subchondral sclerosis development are typical characteristics of late-stage OA [9–11]. In OP, bone loss accelerates in women at menopause due to increased remodeling intensity. Basic multicellular units (BMU) balance becomes increasingly negative due to estrogen deficiency reducing osteoblast lifespan and increasing osteoclast lifespan [5]. Endocortical resorption and accumulating cortical porosity increase the surface available for resorption, thereby leading to accelerated bone loss among elderly men [12].

Abnormal bone remodeling effectuates significant changes to the 3-D microarchitecture of bone tissues. Several studies have been performed using high-resolution peripheral quantitative computed tomography (HR-pQCT) and micro-computed tomography (micro-CT). However, previous reports of cortical thickness and porosity were controversial [13–15]. One in vitro study of the femoral neck revealed that RA cancellous bone had significantly greater BV/TV and surface density (BS/TV) compared to the donor control group, although RA bone tissues exhibited severe erosion [16]. Moreover, other in vitro study revealed that OA femoral neck cancellous bone exhibited significantly greater bone volume fraction, as well as typical plate-like structure and surface density, while OA bone tissue displayed marked osteophyte formation [16,17]. In OP, a high remodeling rate reduces the mineral content of bone tissue. The negative BMU balance resulted in trabecular thinning, the disappearance and loss of connectivity, cortical thinning, and increased intracortical porosity [5].

Over the past three decades, much has been learned regarding the 3-D microarchitectural properties of these diseased bones, which provides significant information on changes in properties among bone tissues [17,18]. There are some published studies comparing femoral head (and neck) trabecular bone microarchitecture and mechanical properties between OA and OP [19,20] as well as between OA and controls [21,22]. Nevertheless, a comprehensive comparison of the microarchitecture of cancellous bones between RA, OA, OP and donor control (CNT) simultaneously is lacking.

Recently, a novel approach to the volumetric spatial decomposition (VSD) of trabeculae from micro-CT images has become available. A 3-D bone structure can be divided into its basic rod and plate elements, thereby allowing the computation of various trabecular morphometric index parameters [23,24]. However, knowledge regarding the rod- and plate-like trabecular morphometric properties of these diseases also remains limited.

As such, the aims of the present study were: 1) to investigate and compare the 3-D microarchitectural properties of cancellous bones in the femoral heads of patients with RA, OA, OP, or donor controls; and 2) to quantify and compare their rod- and plate-like trabecular morphometric properties. We hypothesized that the 3-D microarchitectural properties and rod- and plate-like trabecular morphometric properties would differ significantly among groups, and that they would exhibit different levels of bone quality deterioration.

2. Materials and methods

2.1. Human femoral head samples

This study included femoral head samples harvested during total hip replacement surgery from patients with rheumatoid arthritis (n = 12, male = 4), osteoarthritis (n = 15, male = 4), and osteoporosis (n = 24, male = 7). A total of eight donor controls were also included (male = 4). A strict inclusion criterion was used for selecting samples: (i) Caucasian patients; (ii) the diagnosis of RA, OA, or OP were confirmed by clinical and radiological evidence; and (iii) radiological, biochemical, and histological tests ruling out any other disease (such as congenital or acquired dysplasia, gout, or avascular necrosis) (see Table 1).

Eight control femoral heads were collected at the Department of Neurobiology Research, University of Southern Denmark, from Caucasian donors who donated to anatomical education. Macroscopically, the femoral heads/necks were free from pathological changes, and the articular cartilage was relatively intact. The control donors' medical histories were also checked to exclude any metabolic diseases that might affect bone microarchitecture.

Written informed consent was obtained from all patients who underwent total hip replacements, and from donors to offer cadavers for anatomical education and research. The Department of Orthopedic Surgery and Traumatology, Odense University Hospital, and the Ethic Committee of the Region of Southern Denmark have approved this study (ID: S-VF-20040094).

2.2. Sample preparation

During standard total hip replacement procedures, the femur head was sawed off at the femoral neck based on a preoperative template. The femur head and concomitant femoral neck samples were immediately placed in sealed plastic bags and stored inside glass containers and kept at −20 °C. Prior to further preparation, the samples were placed at room temperature for 2 h to defrost. The femoral heads and necks were carefully cleaned of soft connective tissue using a scalpel. A first saw was made 10 mm from the top of femoral head, and a second saw was made 10 mm distally along the femoral head/neck to obtain a 10 mm thick segment (Fig. 1).

A diamond-coated band saw – the EXAKT-Cutting Grinding System (Exakt Apparatebau GmbH & Co. KG, Norderstedt, Germany) – was used for the sawing procedures at low speed. The aforementioned segments were glued onto a special device and mounted on a saw Microtome 1600 (Ernst Leitz Wetzlar GmbH, Wetzlar, Germany). The samples were continuously irrigated with tap water during sawing (Fig. 1). A total of four cubic cancellous bone samples ($10 \times 10 \times 10$ mm^3) were produced from the standardized locations of each femoral head. The number and orientation of each sample were identified as antero-posterior (AP), medial-lateral (ML), and cephalo-caudal (CC) [25]. After preparation, all the specimens were frozen and stored in sealed plastic tubes at −20 °C until micro-CT scanning or mechanical tests.

Table 1
Age and sex of patients for each group.

Patients/donor	Total	Age (years)		Sex	
		Mean ± SD	Range	male	Female
Rheumatoid arthritis	n = 12	63.1 ± 16.2	29–86	n = 4	n = 8
Osteoarthritis	n = 15	67.5 ± 8.0	53–82	n = 4	n = 11
Osteoporosis	n = 24	82.8 ± 6.2	71–94	n = 7	n = 17
Donor control	n = 8	76.8 ± 11.1	52–92	n = 4	n = 4

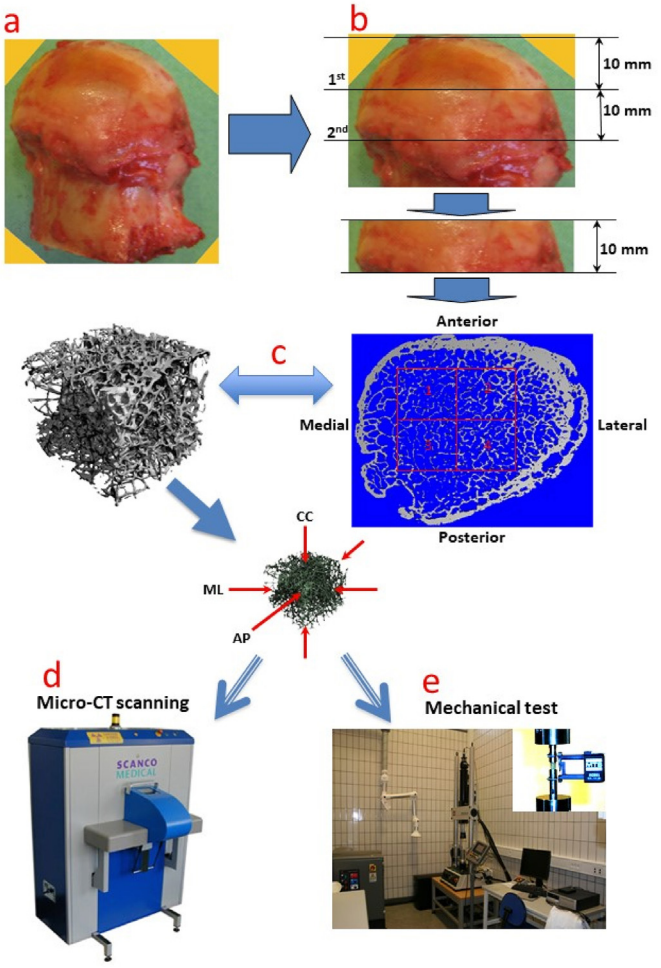

Figure 1. Study design and sample preparation are illustrated. (a) Diseased femoral heads were harvested during total hip replacement surgery. Donor control femoral heads were also collected. (b) The section direction was performed according to the loading axial of the femoral head. The sample was sawed 10 mm from femoral head surface. Then, a second saw was made at 10 mm beneath the first section to produce a 10-mm thick segment using a diamond-coated band saw. (c) Four cubic cancellous bone samples were sawed from each segment. (d) All the samples were micro-CT scanned. 3-D microarchitectural properties and morphometric properties were then quantified. (e) After 10 preconditioning cycles between a preload of 3 N and a strain of 0.006, the samples were further tested in compression to failure in order to determine their mechanical properties.

2.3. Micro-CT scanning

All samples were micro-CT scanned using a high resolution microtomographic system (vivaCT 40, Scanco Medical AG., Brüttisellen, Switzerland) with a voltage of 70 kV and a current of 85 μA. Each 3-D image data set consisted of approximately 800 slices. The scanned images resulted in 3-D reconstruction cubic voxel sizes of 12.5 × 12.5 × 12.5 μm^3 (2048 × 2048 x 2048 pixels) with 32-bit-gray-levels. For field of view, the scan diameter was 2048 pixels x 12.5μm/pixel = 25.6 mm, and the volume was 25.6 × 25.6 × 10.0mm^3. All micro-CT images were segmented by applying the optimal threshold of 210 and using previously described segmentation techniques [26] to obtain accurate 3-D imaging data sets.

2.4. 3-D microarchitectural analysis

The 3-D microarchitectural properties of cubic cancellous bone were calculated using true, unbiased, and assumption-free methods [27–29]. Bone volume fraction (BV/TV, %) was computed as the percentage of bone volume per total specimen volume [26]. Direct trabecular thickness (Tb.Th, μm) was calculated independently of an assumed structure type [29]. Architectural anisotropy (the orientation of trabeculae) was quantified using the mean intercept length method. Degree of anisotropy (DA, -) was determined as the ratio between primary and tertiary eigenvalues [30]. Connectivity density (Conn.D, mm^{-3}), based on a topological approach, measured a multiple connections within trabecular bone [27]. Bone surface density (BS/TV, mm^{-1}) was computed as the percentage of bone surface per total specimen volume, and bone surface to volume ratio (BS/BV, mm^{-1}) was the ratio between bone surface and bone volume. Trabecular separation (TbSp, μm), the mean distance between trabeculae, and trabecular number (TbN, mm^{-1}), and the mean number of trabeculae were also calculated (Fig. 2).

2.5. Local morphometric analysis

To compute morphometric indices at the trabecular level, the VSD of trabecular structures was performed using the techniques developed by Stauber & Muller [23]. From 3-D images, local morphometry – as applied to individual rods and plates – was identified directly. The morphometric measures of individual trabecular elements included the number of rods (Nr.Rods) and the number of plates (Nr.Plates) within the total volume of interest. The rod volume density (Ro.BV/TV) was defined as the total rod volume divided by the total volume of interest in percent, while the plate volume density (Pl.BV/TV) was defined as total plate volume divided by the total volume of interest in percent. The relative bone volume fraction of rods (Ro.BV/BV) and plates (Pl.BV/BV = 100%−Ro.BV/BV) were determined as percentages [23]. The mean volume (<Ro.V>, <Pl.V>), mean surface (<Ro.S>, <Pl.S>), and mean thickness (<Ro.Th>, <Pl.Th>) averaged for each structure over all rods and plates separately were also calculated. The mean orientation (<Ro.θ>; the angle between the orientation of the element and the image axis) and mean longitudinal length (<Ro.Le>, <Pl.Le>) were also computed [23,24]. Structure model index (SMI, -) was defined as a type of cancellous bone whether it was dominated by rods or plates (Fig. 2) [28].

2.6. Compression mechanical test

Prior to testing, the samples were placed at room temperature for 2 h and were kept moist during the experiment. Compression tests were performed on an 858 Bionix MTS hydraulic material testing system (MTS Systems Co., Minneapolis, Minnesota, USA) using a 1 kN load cell. After 10 preconditioning cycles between a preload of 3 N and a strain of 0.006, the samples were tested in compression to failure on the CC direction (i.e. the main loading directions of trabeculae). Mechanical properties such as ultimate stress (strength, MPa), Young's modulus (MPa), ultimate strain (%), and failure energy (kJ/cm^3) were calculated from stress–strain curves converted from the recorded load–deformation curve (Fig. 1) [31].

2.7. Statistical analysis

Entire data sets were used for statistical analyses (SPSS for Windows, version 25, SPSS Inc. Chicago, Illinois, USA), and the mean value for each femoral head derived from four samples was used to compare differences among 4 groups, thus each individual was represented by one set of values. All data were first checked for equal variance and normality. One-way analysis of variance (ANOVA) was used to compare properties

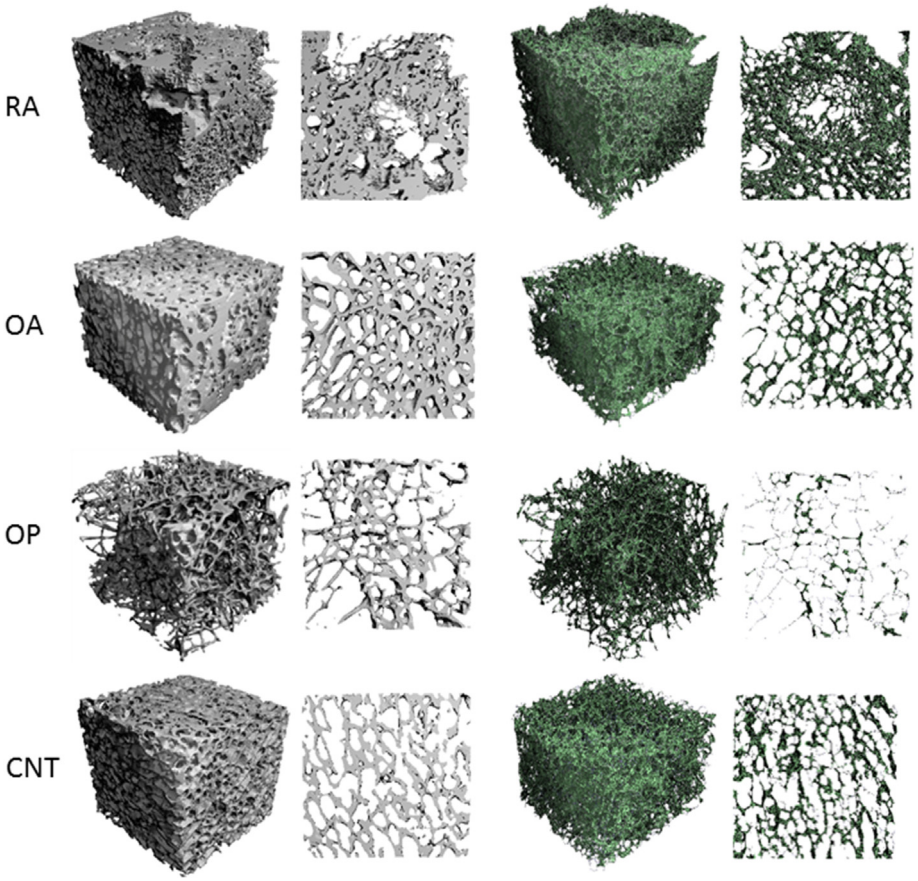

Figure 2. 3-D reconstructions of micro-CT images for the four groups are displayed. Significant differences in the microarchitecture and dominating plate-like, rod-like, or combined trabecular structure can be observed. Noticeably, erosion, irregular structure, and compensated thickening around erosion are apparent in RA samples, while OA samples had thicker and denser trabeculae, and OP trabeculae had poor connection and increased separation compared to the CNT samples.

among the four groups. If the F-test showed a significant level, post-hoc multiple comparisons were made to determine differences between groups. Linear and multiple regression analyses based on the mean value for each femur were used to assess the associations between one of the mechanical properties as a dependent variable and all measured micro-architectural/morphometric properties as explanatory variables. A p-value <0.05 was considered significant.

3. Results

On average, RA patients were 4.4, 19.7, and 14.5 years younger than OA patients, OP patients, and the CNT donors ($p = 0.37$, $p < 0.001$, and $p = 0.08$, respectively). The OA patients were 15.3 and 10.1 years younger than OP patients and CNT donors ($p < 0.001$ and $p = 0.23$, respectively). Moreover, OP patients were 5.2 years older than the CNT donors ($p = 0.79$).

3.1. 3-D microarchitectural properties

The microarchitectural properties of femoral head cancellous bone revealed significant differences among the four groups, with the exception of the RA and OA groups. Bone volume fraction was significantly greater in the RA and OA groups compared to the OP and the CNT groups ($p < 0.001$). Moreover, trabecular thickness was significantly greater in the RA than in the OP group and was also greater in the OA than in the OP and CNT groups ($p < 0.001$). The degree of anisotropy was significantly lower in the RA and OA groups than in the CNT group ($p = 0.001$). Furthermore, connectivity density was significantly greater in the RA than in the OP and CNT groups ($p < 0.001$). Surface density was significantly greater in the RA and OA groups than in the OP group ($p < 0.001$). Surface volume ratio was significantly lower in the RA and OA groups than in the OP and CNT groups ($p < 0.001$). Trabecular separation was significantly lower in the RA and OA groups than in the OP group ($p = 0.001$). Trabecular number was significantly greater in the RA and OA groups than in the OP and CNT groups ($p < 0.001$, Figures 2 and 3).

3.2. Rod- and plate-like trabecular morphometric properties

The rod- and plate-like trabeculae of femoral head cancellous bone exhibited differences among the four groups (Figs. 4 and 5). The number of rods in the RA was significantly greater than in the other three groups ($p = 0.005$). The number of plates, plate volume density, and relative bone volume fraction of plates in the RA and OA groups were significantly greater than those in the OP and CNT groups ($p < 0.001$, $p < 0.001$, and $p = 0.002$, respectively) (Fig. 5). The relative bone volume fraction of rods in the RA and OA groups were significantly lower than in the OP group ($p = 0.002$). Rod surface in the RA group was significantly lower than in the OP group ($p = 0.019$). The mean orientation of rods in the RA group was significantly greater than in the OP group ($p = 0.007$) (Fig. 4). Moreover, the mean longitudinal length of rods, mean volume of plates, mean surface of plates, and mean longitudinal length of plates in the RA and OA groups were significantly lower than in the OP and CNT groups (all $p < 0.001$). The mean orientation of plates in the RA and OA groups were significantly greater than that of the OP group. Structure model index was significantly lower in the RA and OA groups than in the OP group ($p < 0.001$) ($p = 0.002$, Figures 4 and 5).

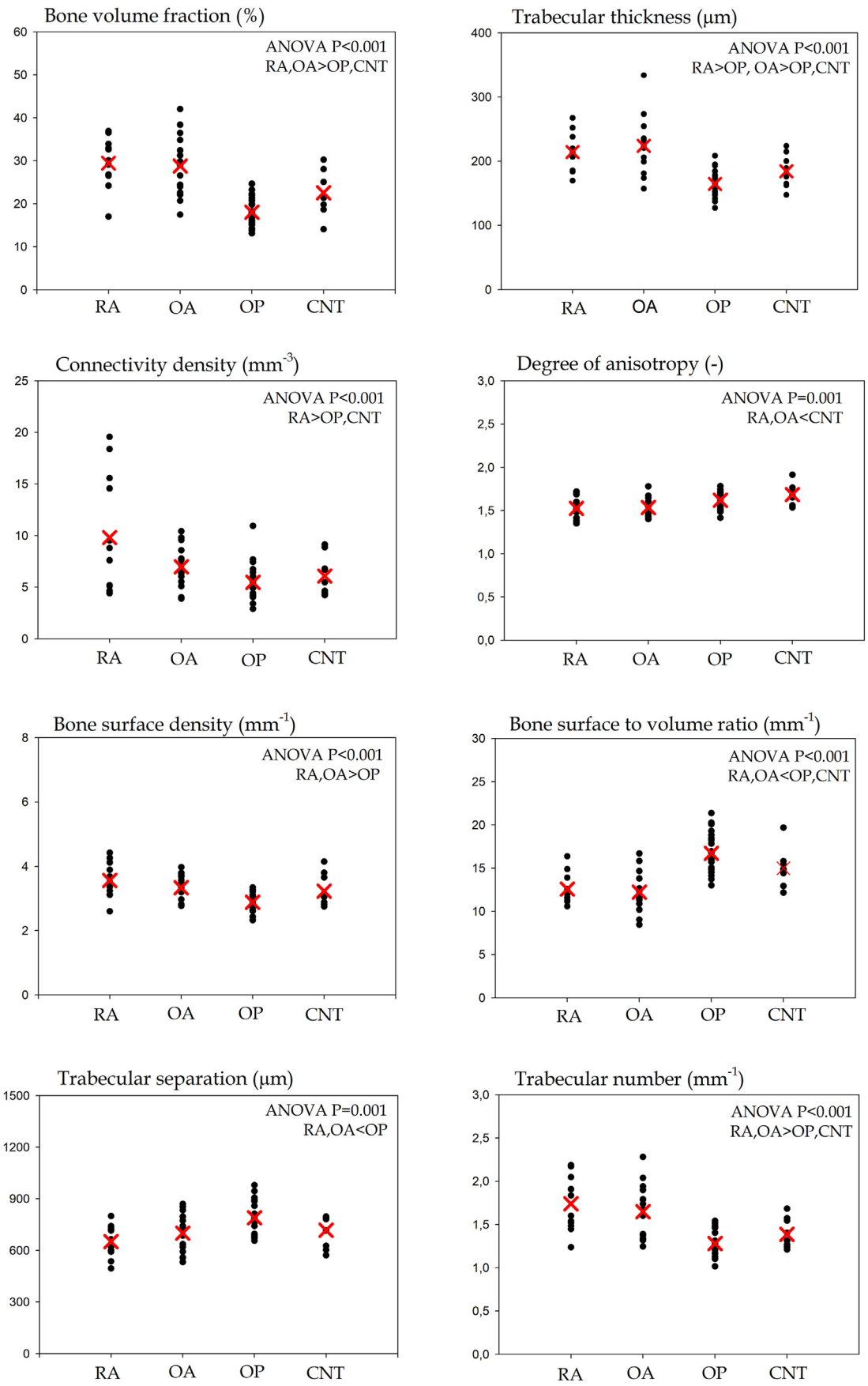

Figure 3. Comparison of 3-D microarchitectural properties among RA, OA, OP and CNT groups. The data are analyzed by ANOVA and displayed by dots with mean values. Significant differences between groups are indicated.

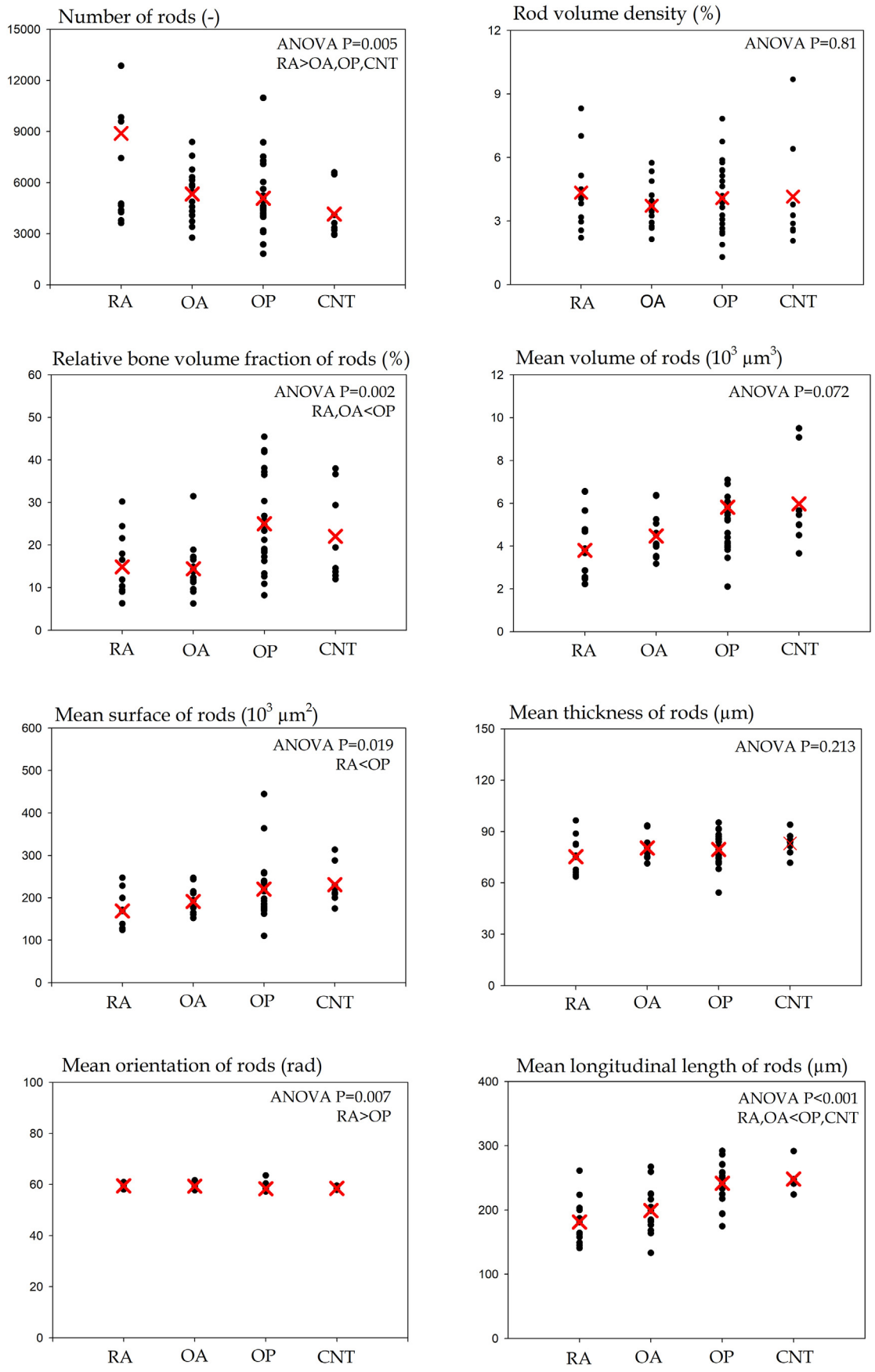

Figure 4. Comparison of 3-D rod-like trabecular morphometric properties among RA, OA, OP and CNT groups. The data are analyzed by ANOVA and displayed by dots with mean values. Significant differences between groups are indicated.

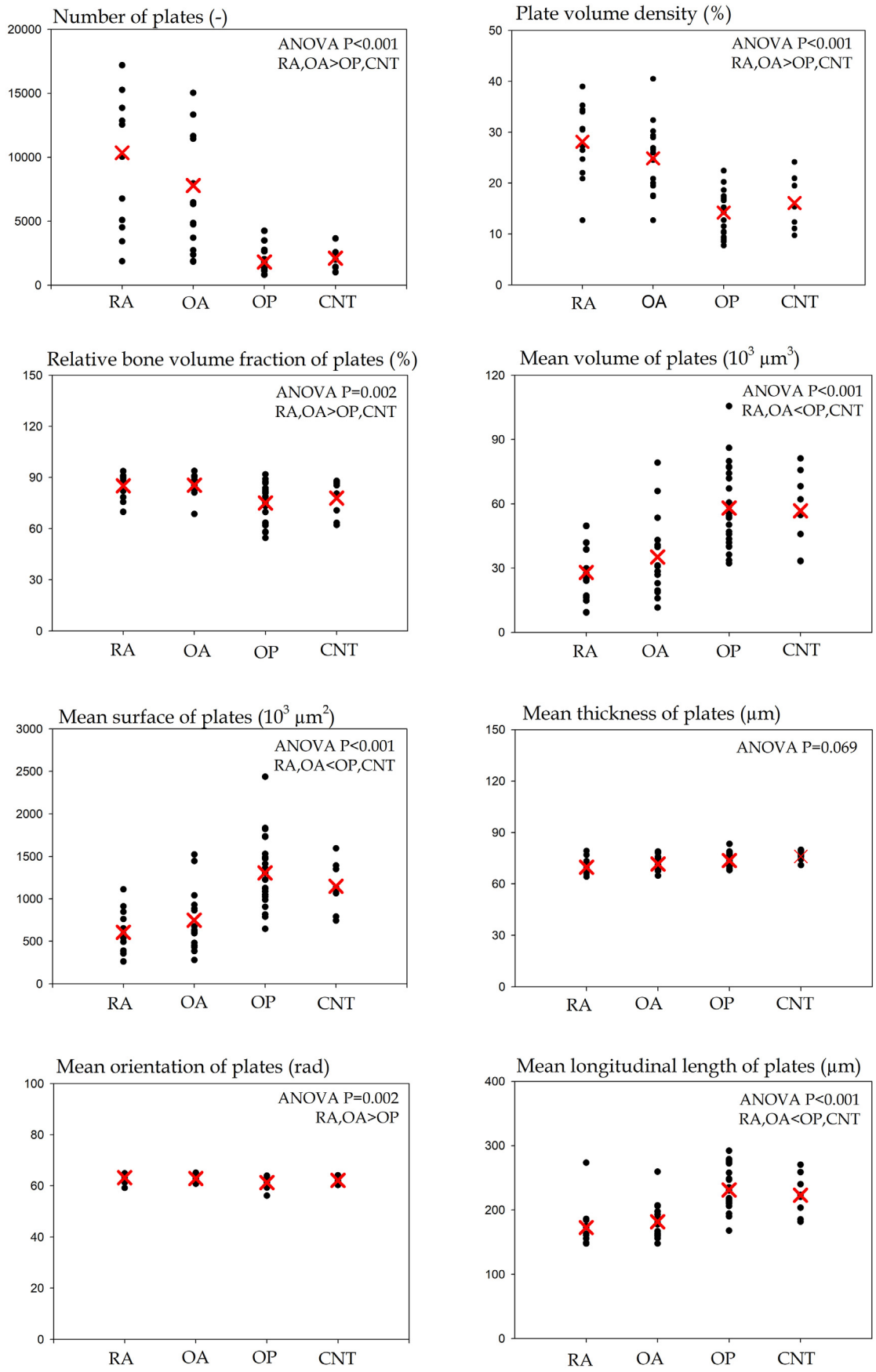

Figure 5. Comparison of 3-D plate-like trabecular morphometric properties among RA, OA, OP and CNT groups. The data are analyzed by ANOVA and displayed by dots with mean values. Significant differences between groups are indicated.

3.3. Mechanical properties and their best determinants

Mechanical properties differed significantly among the four groups. Young's moduli in the RA and OA groups were significantly greater than the OP group by 84% and 127%, respectively. Ultimate stress was 126% and 147% greater in the RA and OA groups, with even the CNT being 77% greater than the OP group, respectively. Failure energy was 298% and 291% greater in the RA and the OA groups than in the OP group, respectively. Ultimate strain in the OA and CNT groups were significantly greater than in the OP group (all $p < 0.001$, Fig. 6).

For the entire data set, the best determinant for mechanical properties was bone volume fraction or structure model index. Bone volume fraction explained 47% of Young's modulus variation and 75% of ultimate stress variation, while the mean orientation of plates and structure model index increased the explanations of ultimate stress to 77.7% and 79.4%, respectively. Structure model index explained 52% of failure energy variation, while rod volume density and mean volume of rods increased this explanation to 61.7% and 64.7%, respectively. The specific determinants for mechanical properties varied between groups.

4. Discussion

The current study investigates the rod- and plate-like trabecular morphometric properties of RA, OA and OP cancellous bone compared to CNT with quantification of the microarchitectural properties of cancellous bone. This study has demonstrated significant differences in the 3-D microarchitectural properties and rod- and plate-like trabecular morphometric properties among patients with RA, OA, and OP, which reflect different degrees of microarchitectural deteriorations in bone quality. Mechanical properties in the RA and OA groups were significantly greater than those of in the OP group. Bone volume fraction was the single strongest predictor of mechanical properties, while morphometric parameters improved the explanations.

Bone volume fractions in RA and OA group femoral heads were significantly greater than those of the OP and CNT groups. Apparently, RA and OA progression attempted to maintain bone tissues, although they were degenerative bone with microdamage and denatured collagen [9,17,32]. This process was opposite to human aging-induced bone loss and osteoporosis. Consequently, the RA and the OA cancellous bone became more plate-like, with thicker trabeculae and increased surface density than the OP cancellous bone. A decreased degree of anisotropy indicated trabeculae were more isotropic in the RA and OA than in the CNT group. The increased bone density also resulted in decreased bone surface/volume ratio and narrowed trabecular separation in the RA and OA groups compared to the OP and the CNT groups. The RA and the OA groups exhibited greater trabecular numbers compared to the OP and the CNT group, while the RA group exhibited a greater connectivity density than the CNT group. This change can be explained by the maintenance of connectivity density and trabecular number in RA and OA, and loss of trabeculae due to aging and OP disease progression.

Interestingly, significant differences in 3-D microarchitectures were observed among the four groups, though not between the RA and OA groups in any parameters measured. No observed differences in the microarchitectural parameters between the RA and OA groups suggested a similar trend of global bone microarchitectural degeneration in these two diseases, though local marked variations cannot be neglected. These

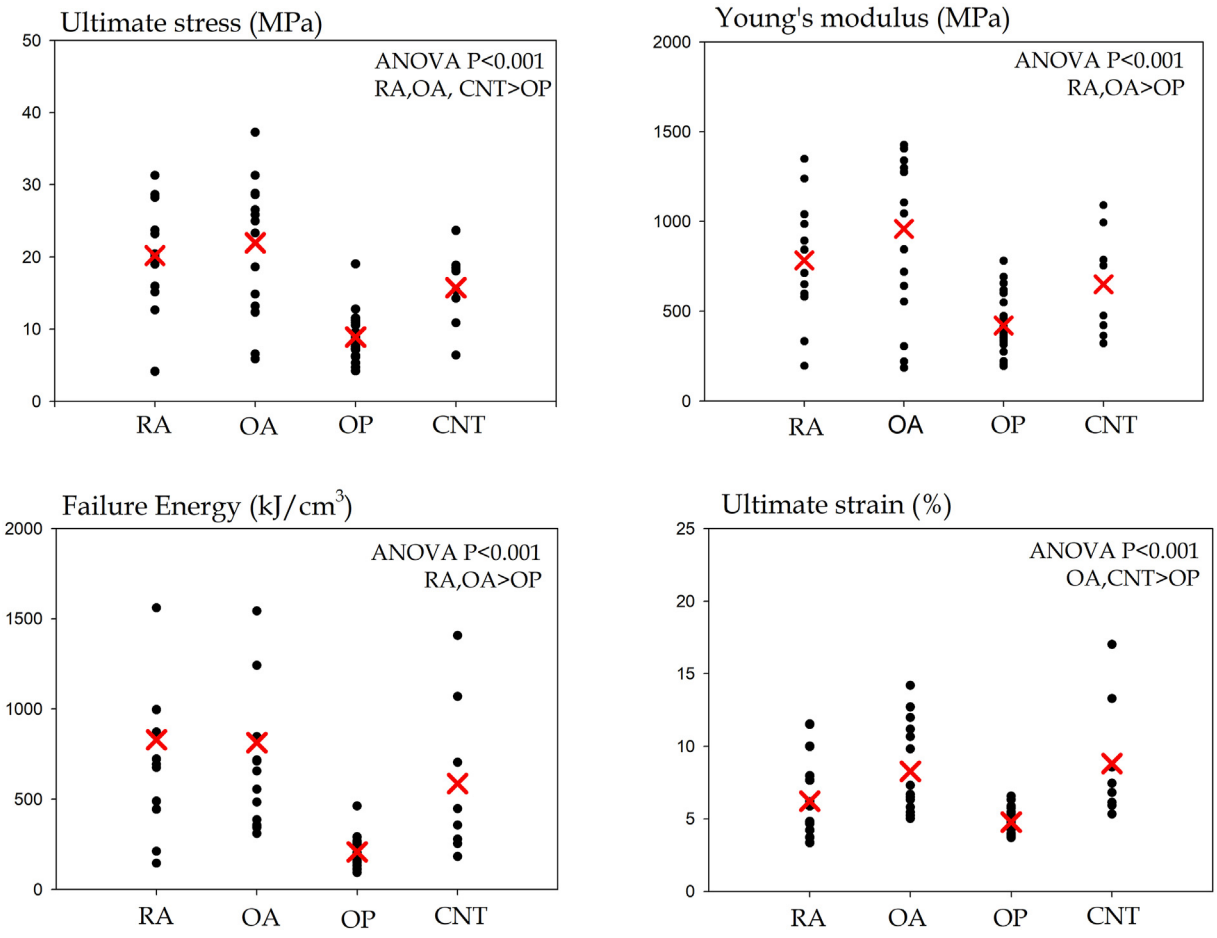

Figure 6. Comparison of mechanical properties among RA, OA, OP and CNT groups. The data are displayed by dots with mean values. Significant differences between groups are indicated.

results are consistent with our previous finding in the RA and OA femoral neck [16]. This is also in line with a previous report highlighting that the periarticular bone had similar microarchitecture and bone remodeling characteristics in RA and OA [33]. Several HR-pQCT studies have reported changes in microarchitecture with the decreased bone volume fraction of periarticular and non-periarticular bone in RA patients [14,15,34] with compromised mechanical strength. These studies are typically on the distal radius [14,15], metacarpal head [7,8], metacarpal shaft [35] and metacarpophalangeal joints [34,36,37].

Our results partial support previous published studies that have compared femoral head (and neck) trabecular bone microarchitecture and mechanical properties between OA and OP [19,20,38,39]. Blain et al. found that the loss of the trabecular bone mass and connectivity in femoral neck plays a role in the skeletal fragility associated with hip fracture in addition to the cortical thinning, and the spatial distribution of the trabeculae differs between OP and OA [19]. Montoya et al. reported that the mechanical properties were worse in OP patients compared to OA, bone turnover markers, bone mineral density, and bone microstructural changes in osteoporosis are opposite to those of OA [20]. Other studies reported the changes in microarchitectural properties in OA relative to the controls [21,22]. More recently, Ryan et al. report an approach to study the heterogeneous properties of OA femoral head [22]. However, investigations on changes to the microarchitecture of the femoral head in RA are limited and provide inconsistent results.

Morphometric analysis of rod- and plate-like trabeculae has provided important insight into the structural element differences of cancellous bone [23,24,40,41]. In the present study, the number of rods and plates was markedly greater in the RA group than in the OP and CNT groups, while the number of plates was significantly greater in the OA group than in the OP and the CNT groups as a result of maintaining bone tissues in the OA and bone loss in the OP and the CNT. Plate volume density in the RA and OA groups were 56%–98% greater than in the OP and the CNT, respectively, suggesting a typical plate-like structure in the RA and OA groups. The relative bone volume fraction of rods in the RA and OA groups was approximately 40% lower than in the OP group, but the relative bone volume fraction of plates in the RA and OA groups were 9.2–14% greater than in the OP and CNT groups, thereby suggesting the RA and OA groups were dominated by plate-like trabeculae by 85% while the OP and the CNT groups exhibited rich rod-like trabeculae despite also being dominated by plate-like trabeculae by 75% (Figs. 4 and 5).

Morphometric changes in the RA and OA groups are accompanied by shorter mean longitudinal length of rods than the OP and CNT groups, with RA being accompanied by a relatively lower mean surface of rods and a greater mean orientation of rods in the RA than in the OP group. Moreover, morphometric changes in the RA and OA groups also accompany a lower mean volume and surface of plates, as well as a shorter mean longitudinal length of plates than in the OP and CNT groups. Similar to microarchitecture, no differences in rod- and plate-like trabecular parameters were observed between the RA and the OA, apart from the number of rods, which suggests a similar pattern of bone remodeling during the disease process that changed the morphometry of trabecular elements.

Significant differences in mechanical properties were observed between groups (Fig. 6). OP cancellous bone was the weakest among all four cancellous bones. The greater mechanical properties in the RA and OA groups were consistent with their greater bone volume fraction. Notably, similar mechanical properties were observed between the RA and OA groups, reflecting similar bone volume fractions among these two diseased bone tissues. Furthermore, markedly greater observed strength in the RA and OA groups than the OP group clearly indicates fracture incidence frequently occurring in the OP group [6].

Our study has several limitations. First, the mean ages of the RA and OA patients were lower than those of the OP patients (both $p < 0.001$). As such, aging-related influence on microarchitecture could not be eliminated. Second, sample size was relatively small. Third, differing sex ratios might explain some of the variations within and between groups. Therefore, the results should be interpreted with caution. The strengths of this study include: 1) simultaneously investigated rod- and plate-like trabecular element level morphometric properties and 3-D microarchitectural level properties of RA, OA, and OP cancellous bones; 2) revealing the differences in changes to properties leading to different bone microarchitectural degeneration patterns.

In conclusion, our study has demonstrated significant differences in 3-D microarchitecture as well as rod- and plate-like trabecular morphometric properties among RA, OA, and OP femur head cancellous bone. RA and OA cancellous bone displayed similar patterns of bone microarchitectural degeneration and pronounced different microarchitectures from the OP, despite apparent bone erosion in RA, marked osteophyte formation in OA, and severe bone loss in OP cancellous bone. The OP group exhibited the weakest cancellous bone strength, while the RA and OA groups exhibited a compensatory effect that maintains bone tissues, and hence mechanical properties – although with poor bone quality [42].

Author contributions

M Ding: Conceptualized and designed the study; Funding acquisition; Performed the study; Collected, analyzed, and interpreted the data; Wrote and revised the manuscript. S Overgaard: Conceptualized and designed the study, Reviewed the manuscript. Both authors read and approved the final manuscript.

Declaration of competing interest

The authors have no conflict of interest to declare.

Acknowledgements

We thank Gitte Højlund Reinberg and Jakob Danielsen for skillful technical assistance, and chief consultants Jens Ole Laursen and Ole Ovesen for providing the osteoarthritis samples. This study was kindly supported by the research grants from the Danish Council for Independent Research – Medical Sciences (DFF– 4004–00256, MD), Region of Southern Denmark (08/17871 and 15/2485, MD), and the Danish Rheumatism Association.

References

[1] Smolen JS, Aletaha D, Barton A, Burmester GR, Emery P, Firestein GS, et al. Rheumatoid arthritis. Nat. Rev. Dis. Primers 2018;4:18001.
[2] Dieppe PA, Lohmander LS. Pathogenesis and management of pain in osteoarthritis. Lancet 2005;365(9463):965–73.
[3] ConsensusDevelopmentConference. Prophylaxis and treatment of osteoporosis. Am J Med 1991;90(1):107–10.
[4] Sinigaglia L, Varenna M, Girasole G, Bianchi G. Epidemiology of osteoporosis in rheumatic diseases. Rheum Dis Clin N Am 2006;32(4):631–58.
[5] Seeman E. Reduced bone formation and increased bone resorption: rational targets for the treatment of osteoporosis. Osteoporos Int 2003;14(Suppl 3):S2–8.
[6] Black DM, Rosen CJ. Postmenopausal Osteoporosis, N. Engl. J. Med 2016;374(21): 2096–7.
[7] Baum R, Gravallese EM. Bone as a target organ in rheumatic disease: impact on osteoclasts and osteoblasts. Clin Rev Allergy Immunol 2016;51(1):1–15.
[8] Werner D, Simon D, Englbrecht M, Stemmler F, Simon C, Berlin A, et al. Early changes of the cortical micro-channel system in the bare area of the joints of patients with rheumatoid arthritis. Arthritis Rheum 2017;69(8):1580–7.
[9] Burr DB, Gallant MA. Bone remodelling in osteoarthritis. Nat Rev Rheumatol 2012; 8(11):665–73.
[10] Felson DT, Neogi T. Osteoarthritis: is it a disease of cartilage or of bone? Arthritis Rheum 2004;50(2):341–4.
[11] Felson DT, Neogi T. Emerging treatment models in rheumatology: challenges for osteoarthritis trials. Arthritis Rheum 2018;70(8):1175–81.
[12] Seeman E. Osteoporosis in men. Bailliere's Clin Rheumatol 1997;11(3):613–29.
[13] Paccou J, Edwards M, Moss C, Dennison E, Cooper C. High-resolution imaging of bone and joint architecture in rheumatoid arthritis. Br Med Bull 2014;112(1): 107–18.
[14] Zhu TY, Griffith JF, Qin L, Hung VW, Fong TN, Au SK, et al. Alterations of bone density, microstructure, and strength of the distal radius in male patients with rheumatoid arthritis: a case-control study with HR-pQCT. J Bone Miner Res 2014; 29(9):2118–29.

[15] Kocijan R, Finzel S, Englbrecht M, Engelke K, Rech J, Schett G. Decreased quantity and quality of the periarticular and nonperiarticular bone in patients with rheumatoid arthritis: a cross-sectional HR-pQCT study. J Bone Miner Res 2014; 29(4):1005–14.
[16] Wang B, Overgaard S, Chemnitz J, Ding M. Cancellous and cortical bone microarchitectures of femoral neck in rheumatoid arthritis and osteoarthritis compared with donor controls. Calcif Tissue Int 2016;98(5):456–64.
[17] Ding M. Microarchitectural adaptations in aging and osteoarthrotic subchondral bone issues. Acta Orthop Suppl 2010;81(340):1–53.
[18] Muller R. Hierarchical microimaging of bone structure and function. Nat Rev Rheumatol 2009;5(7):373–81.
[19] Blain H, Chavassieux P, Portero-Muzy N, Bonnel F, Canovas F, Chammas M, et al. Cortical and trabecular bone distribution in the femoral neck in osteoporosis and osteoarthritis. Bone 2008;43(5):862–8.
[20] Montoya MJ, Giner M, Miranda C, Vazquez MA, Caeiro JR, Guede D, et al. Microstructural trabecular bone from patients with osteoporotic hip fracture or osteoarthritis: its relationship with bone mineral density and bone remodelling markers. Maturitas 2014;79(3):299–305.
[21] Djuric M, Zagorac S, Milovanovic P, Djonic D, Nikolic S, Hahn M, et al. Enhanced trabecular micro-architecture of the femoral neck in hip osteoarthritis vs. healthy controls: a micro-computer tomography study in postmenopausal women. Int Orthop 2013;37(1):21–6.
[22] Ryan M, Barnett L, Rochester J, Wilkinson JM, Dall'Ara E. A new approach to comprehensively evaluate the morphological properties of the human femoral head: example of application to osteoarthritic joint. Sci Rep 2020;10(1):5538.
[23] Stauber M, Muller R. Volumetric spatial decomposition of trabecular bone into rods and plates–a new method for local bone morphometry. Bone 2006;38(4):475–84.
[24] Stauber M, Rapillard L, van Lenthe GH, Zysset P, Muller R. Importance of individual rods and plates in the assessment of bone quality and their contribution to bone stiffness. J Bone Miner Res 2006;21(4):586–95.
[25] Ding M, Danielsen CC, Hvid I, Overgaard S. Three-dimensional microarchitecture of adolescent cancellous bone. Bone 2012;51(5):953–60.
[26] Ding M, Odgaard A, Hvid I. Accuracy of cancellous bone volume fraction measured by micro-CT scanning. J Biomech 1999;32:323–6.
[27] Odgaard A, Gundersen HJ. Quantification of connectivity in cancellous bone, with special emphasis on 3-D reconstructions. Bone 1993;14(2):173–82.
[28] Hildebrand T, Rüegsegger P. Quantification of bone microarchitecture with the structure model index. CMBBE 1997;1:15–23.
[29] Hildebrand T, Rüegsegger P. A new method for the model-independent assessment of thickness in three-dimensional images. J Microw 1997;185:67–75.
[30] Odgaard A, Jensen EB, Gundersen HJ. Estimation of structural anisotropy based on volume orientation. A new concept. J Microsc 1990;157(Pt 2):149–62.
[31] Ding M, Dalstra M, Danielsen CC, Kabel J, Hvid I, Linde F. Age variations in the properties of human tibial trabecular bone. J. Bone Joint Surg. Br 1997;79(6): 995–1002.
[32] Bailey AJ, Mansell JP, Sims TJ, Banse X. Biochemical and mechanical properties of subchondral bone in osteoarthritis. Biorheology 2004;41(3–4):349–58.
[33] Li G, Ma Y, Cheng TS, Landao-Bassonga E, Qin A, Pavlos NJ, et al. Identical subchondral bone microarchitecture pattern with increased bone resorption in rheumatoid arthritis as compared to osteoarthritis. Osteoarthritis Cartilage 2014; 22(12):2083–92.
[34] Figueiredo CP, Kleyer A, Simon D, Stemmler F, d'Oliveira I, Weissenfels A, et al. Methods for segmentation of rheumatoid arthritis bone erosions in high-resolution peripheral quantitative computed tomography (HR-pQCT). Semin Arthritis Rheum 2018;47(5):611–8.
[35] Feehan L, Buie H, Li L, McKay H. A customized protocol to assess bone quality in the metacarpal head, metacarpal shaft and distal radius: a high resolution peripheral quantitative computed tomography precision study. BMC Muscoskel Disord 2013; 14:367.
[36] Kleyer A, Finzel S, Rech J, Manger B, Krieter M, Faustini F, et al. Bone loss before the clinical onset of rheumatoid arthritis in subjects with anticitrullinated protein antibodies. Ann Rheum Dis 2014;73(5):854–60.
[37] Peters M, van den Bergh JP, Geusens P, Scharmga A, Loeffen D, Weijers R, et al. Prospective follow-up of cortical interruptions, bone density, and micro-structure detected on HR-pQCT: a study in patients with rheumatoid arthritis and healthy subjects. Calcif Tissue Int 2019;104(6):571–81.
[38] He Z, Chu L, Liu X, Han X, Zhang K, Yan M, et al. Differences in subchondral trabecular bone microstructure and finite element analysis-based biomechanical properties between osteoporosis and osteoarthritis. Journal of orthopaedic translation 2020;24:39–45.
[39] Chu L, He Z, Qu X, Liu X, Zhang W, Zhang S, et al. Different subchondral trabecular bone microstructure and biomechanical properties between developmental dysplasia of the hip and primary osteoarthritis. Journal of orthopaedic translation 2020;22:50–7.
[40] Liu XS, Sajda P, Saha PK, Wehrli FW, Bevill G, Keaveny TM, et al. Complete volumetric decomposition of individual trabecular plates and rods and its morphological correlations with anisotropic elastic moduli in human trabecular bone. J Bone Miner Res 2008;23(2):223–35.
[41] Ding M, Lin X, Liu W. Three-dimensional morphometric properties of rod- and plate-like trabeculae in adolescent cancellous bone. Journal of orthopaedic translation 2018;12:26–35.
[42] Ding M, Odgaard A, Hvid I. Changes in the three-dimensional microstructure of human tibial cancellous bone in early osteoarthritis. J Bone Joint Surg Br 2003; 85(6):906–12.